AIP | Applied Physics Letters

Ballistic thermal transport in monolayer transition-metal dichalcogenides: Role of atomic mass

Jinlong Ma, Wu Li, and Xiaobing Luo

Citation: Applied Physics Letters **108**, 082102 (2016); doi: 10.1063/1.4942451
View online: http://dx.doi.org/10.1063/1.4942451
View Table of Contents: http://scitation.aip.org/content/aip/journal/apl/108/8?ver=pdfcov
Published by the AIP Publishing

Ballistic thermal transport in monolayer transition-metal dichalcogenides: Role of atomic mass

Jinlong Ma,[1] Wu Li,[2,a)] and Xiaobing Luo[1,b)]
[1]*State Key Laboratory of Coal Combustion, School of Energy and Power Engineering, Huazhong University of Science and Technology, Wuhan 430074, China*
[2]*CEA-Grenoble, 17 Rue des Martyrs, Grenoble 38000, France*

(Received 18 November 2015; accepted 8 February 2016; published online 22 February 2016)

We investigate the ballistic thermal transport of monolayer transition-metal dichalcogenides (TMDs), which is crucial for the thermal management of their potential applications in nanoelectronics. We find the thermal conductance is mainly affected by the atomic masses of TMDs. As a consequence, the temperature dependences of thermal conductances of different TMDs cross: At low temperatures below ~50 K, the thermal conductance increases with the atomic mass, while it exhibits the opposite trend at high temperatures. The crossing behavior of temperature dependent thermal conductance is characteristic of the atomic mass effect, and TMDs provide a model system demonstrating that the thermal conductance can be effectively manipulated via the atomic mass by selecting appropriate atom. In addition, we clarify that in any two dimensional system such as monolayer TMDs and graphene, due to quadratic dispersion of the out-of-plane modes, the thermal conductance and specific heat in the low temperature limit are proportional to $T^{3/2}$ and T, respectively. Mainly because of much smaller group velocities of in-plane acoustic phonons, the high temperature thermal conductances of monolayer TMDs are much smaller than graphene. However, due to comparable group velocities of out-of-plane acoustic phonons, below 100 K thermal conductances of monolayer TMDs are rather comparable to graphene if taking the same layer thickness for comparison. © *2016 AIP Publishing LLC*. [http://dx.doi.org/10.1063/1.4942451]

The monolayer transition-metal dichalcogenides (TMDs) open up great opportunities for the applications of two dimensional (2D) materials[1] in transistor,[2–4] photodetectors,[5–7] and electroluminescence and photoluminescence devices.[8–10] In these devices, the thermal conductivity determines the efficiency of heat dissipation, which is crucial for the device performance and reliability. Based on first-principles calculations,[11] one of the authors and coworkers have showed the room temperature thermal conductivity of monolayer MoS_2 is larger than 83 $W\,m^{-1}\,K^{-1}$ for 1 μm sample, which has been confirmed by latter experiments[12,13] and calculations.[14] When the size of sample is much smaller than the mean free paths, phonons can conduct heat without being scattered, known as ballistic regime.[15–17] The results on large samples demonstrate that at room temperature phonon mean free paths of TMDs can be hundreds of nanometers.[11,14] Therefore, the ballistic transport occurs in TMDs devices with lengths of tens of nanometers or less. For instance, for MoS_2, the ballistic transport can persist up to 30 nm at room temperature[14] and up to larger lengths at lower temperatures. Despite the great significance and relevance in thermal management of devices based on these 2D materials, the systematic investigation of ballistic thermal conductance of monolayer TMDs is still lacking.

In this work, the ballistic thermal conductance and specific heat of monolayer MoS_2, WS_2, $MoSe_2$, and WSe_2 are studied from the first-principles calculation. We reveal that the ballistic thermal conductance is mainly affected by the atomic masses of TMDs, leading to characteristic crossing of the temperature dependent conductances, and demonstrating the thermal conductance can be effectively manipulated via the atomic mass. Additionally, the difference in thermal conductance between monolayer TMDs and graphene is also elucidated.

The interatomic force constants (IFCs) of monolayer TMDs are obtained by using Vienna *Ab-initio* Simulation Package (VASP)[18] with projector augmented wave (PAW) pseudopotentials[19] and local density approximation (LDA) to the exchange-correlation functional[20] and Phonopy[21] based on the real-space supercell approach.[22] The geometry relaxation is done for the unit cell with a $12 \times 12 \times 1$ grids of $\mathbf{k}$ and a vacuum space along c-axis is fixed to 20 Å to eliminate the interaction arising from periodic boundary condition calculation. A $6 \times 6 \times 1$ supercell with $2 \times 2 \times 1$ $\mathbf{k}$ sampling is used for IFCs calculation. We notice that as the raw IFCs do not satisfy all symmetries, the out-of-plane acoustic (ZA) branch around the Γ point is linear rather than theoretically quadratic, as can be found in previous first-principles calculations on 2D systems.[14,23–34] Here, the IFCs are further symmetrized using a just developed "by construction" approach,[35] correctly giving quadratic phonon dispersion for ZA modes, ensuring the accuracy of calculation especially at low temperatures. For the calculations of thermal conductance and specific heat, a $1200 \times 1200 \times 1$ meshes of $\mathbf{q}$ is used to guarantee the convergence down to 1 K.

Once the phonon dispersion is obtained, the ballistic thermal conductance can be calculated as[36,37]

$$\sigma(T) = \frac{1}{NV}\sum_{p,\mathbf{q}} \frac{\partial f}{\partial T}(\hbar\omega_{p,\mathbf{q}})\frac{|v^x_{p,\mathbf{q}}|}{2}, \tag{1}$$

where the phonon mode is labeled by the branch index p and wavevector $\mathbf{q}$. $\omega_{p,\mathbf{q}}$ is the angular frequency and $v^x_{p,\mathbf{q}}$ is the

a)Electronic mail: wu.li.phys2011@gmail.com
b)Electronic mail: luoxb@hust.edu.cn

group velocity along the x direction, in which the thermal conductance is investigated. $\hbar$ is the reduced Planck's constant and f is the equilibrium Bose-Einstein distribution. N is the number of uniformly spaced $\mathbf{q}$ points in the Brillouin zone, and V is the volume of unit cell. Since V is not a well-defined quantity in 2D system, for convenience, a constant thickness $H = 6.033$ Å is applied to all monolayer TMDs, which is equal to the layer separation in bulk MoS_2.[11] Although $\sigma(T)$ depends on the transport direction x, we find the anisotropy of $\sigma(T)$ in monolayer TMDs is smaller than 0.7%, in agreement with the small anisotropy for graphene;[38] therefore, $\sigma(T)$ can be considered as isotropic in monolayer TMDs. Note that the specific heat per unit volume c_V (T), which is closely related to $\sigma(T)$, can be obtained from the right-hand side of Eq. (1) by excluding the factor of $\frac{|v^x_{p,\mathbf{q}}|}{2}$.[22,39,40]

The calculated lattice constants of monolayer MoS_2, WS_2, $MoSe_2$, and WSe_2 are 3.118 Å, 3.126 Å, 3.244 Å, and 3.249 Å, respectively, in good agreement with experimental data[41–44] and other calculations.[11,14,24] The calculated phonon dispersions are plotted in Fig. 1(a). It can be seen that these phonon dispersions exhibit similar shapes, and the relative differences in optical phonons are on average larger than those in acoustic phonons. Note that quadratic dispersions are obtained for the ZA branch around Γ point, in contrast to the other calculations.[14,23–34] The phonon dispersion is mainly determined by the harmonic IFCs and the atomic mass. Figure 1(a) indicates the compounds with larger atomic masses have smaller phonon frequencies. We find that the difference in the phonon dispersion, especially for the low frequency phonons, is actually dominated by the atomic mass difference. As can be seen in Fig. 1(b), if artificially changing the atomic mass of Se to that of S, and the mass of W to that of Mo, the phonon dispersion of WS_2, $MoSe_2$ and WSe_2 become very close to that of MoS_2. Specifically, in the case that only the cation differs, the remaining discrepancy between MoS_2 and WS_2 or between $MoSe_2$ and WSe_2 is smaller than 7% for both acoustic and optical phonons. In the case that the anion differs, i.e., MoS_2 vs $MoSe_2$ or WS_2 vs WSe_2, the remaining difference for optical phonons is still below 8%, but for acoustic phonons, the difference is up to a maximum of 20% at some $\mathbf{q}$. However, comparing with the differences in the original phonon dispersions, as shown in Fig. 1(a), these discrepancies resulting from factors other than the atomic mass are rather insignificant. This means the harmonic IFCs have good transferability among these systems, especially when only the cation differs. The larger discrepancy found in the case that the anion differs can be attributed to the larger lattice mismatch.[45]

Despite the fact that the phonon dispersion obeys D_{6h} point group symmetry, the zone-center acoustic phonons are nearly isotropic. As an example, the $\mathbf{q}$ dependence of the frequencies around Γ point of monolayer MoS_2 are plotted in Fig. 2. It is evident that at short wavevector the frequencies are independent of the polar angle θ of $\mathbf{q}$, while there exists a $\pi/3$ periodicity at large wavevector, as clearly shown in Fig. 2(d). Then, the zone-center phonons can be well described with $\omega = v_{\mathrm{TA/LA}}\, q$ for in-plane transverse acoustic (TA) and longitudinal acoustic (LA) branches, and $\omega = \alpha_{\mathrm{ZA}}\, q^2$ for the ZA branch, where $v_{\mathrm{TA/LA}}$ and α_{ZA} are independent of the direction of $\mathbf{q}$. The calculated values of $v_{\mathrm{TA/LA}}$ and α_{ZA} of monolayer TMDs are listed in Table I, clearly showing that they decrease with increasing atomic mass. Although the masses of the two constituent elements are not uniformly scaled in different compounds, the change of zone-center acoustic phonons depends on the total atomic mass. Since the change of the phonon dispersion is dominated by the change of atomic mass, $v_{\mathrm{TA/LA}}$ and α_{ZA} approximately scale as $1/\sqrt{M_{uc}}$, where M_{uc} denotes the relative atomic mass in the unit cell. As can be seen in Fig. 1(a), the influence of atomic mass on optical phonons can be even larger than the change of $1/\sqrt{M_{uc}}$.

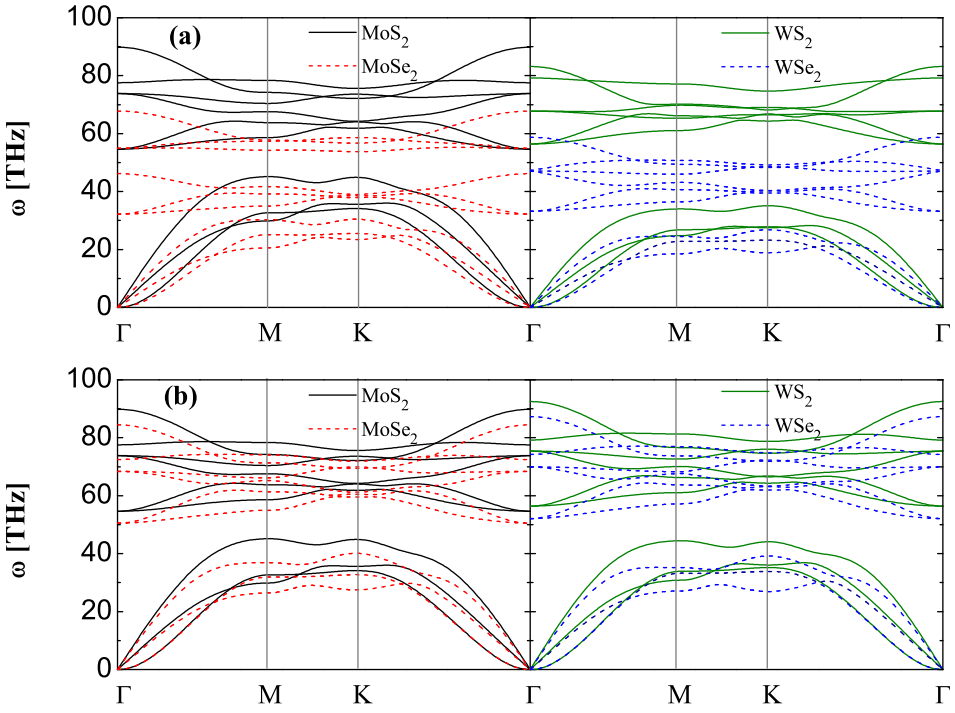

FIG. 1. (a) Calculated phonon dispersions of monolayer MoS_2, WS_2, $MoSe_2$, and WSe_2. (b) Calculated phonon dispersions with the atomic masses of W and Se replaced with those of Mo and S, respectively.

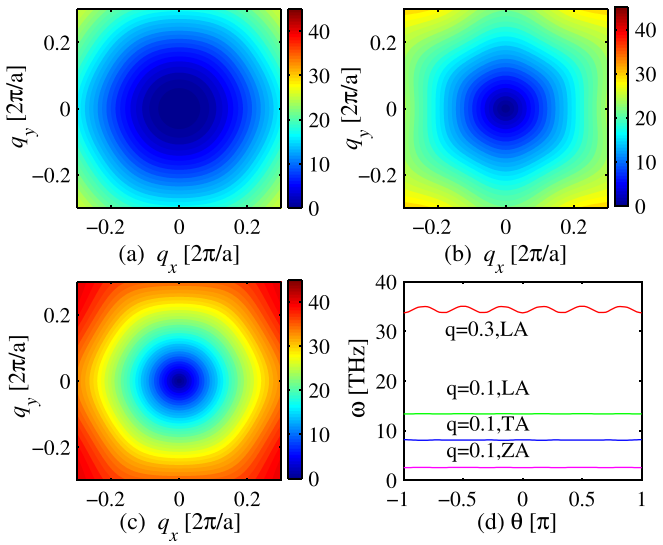

FIG. 2. The frequency distribution of (a) ZA, (b) TA and (c) LA of monolayer MoS_2 depending on **q**, in unit of $2\pi/a$ with a being the lattice constant. (d) The angular dependence of the frequency at $q = 0.1$ and $q = 0.3$.

Figure 3 presents the temperature dependences of σ and c_V for monolayer MoS_2, WS_2, $MoSe_2$, and WSe_2. The temperature dependences of σ and c_V result from the mode specific heat capacity $\frac{\partial f}{\partial T}(\hbar\omega_{p,\mathbf{q}})$. At high temperatures, all phonon modes are effectively excited, and the mode specific heat capacity approaches to the classic limit k_B. Therefore, at high temperatures, both σ and c_V become constant. The constant c_V only depends on the volume of the unit cell. As the lattice constants and volumes are quite similar, the constant c_V is nearly the same for all monolayer TMDs systems. Comparing to c_V, the σ is additionally affected by the group velocity. Due to the fact that compounds with smaller atomic masses tend to have larger group velocities on average, σ at high temperature are larger in those compounds with smaller atomic mass.

In the low temperature limit, only phonons with $\hbar\omega < k_BT$ are well excited and contribute to σ and c_V. Therefore, σ and c_V decrease with decreasing temperature. The low frequency acoustic phonons determine the low temperature limit. Since low frequency acoustic phonons are isotropic, σ and c_V in the low temperature limit can be derived analytically

TABLE I. The relevant qualities of monolayer TMDs and graphene. The relative atomic mass M_{uc} and lattice constant a (Å) of unit cell. v_{LA} (10^3 m/s), v_{TA} (10^3 m/s), and α_{ZA} (10^{-7} m^2/s) characterizing the low frequency phonon dispersions. The low temperature thermal conductance and specific heat contributed from TA + LA branches $\sigma^{\mathrm{low}}_{\mathrm{TA+LA}}$ (10^5 W m^{-2} K^{-3}), $c^{\mathrm{low}}_{V,\mathrm{TA+LA}}$ (10^3 J m^{-3} K^{-3}), and from ZA branch $\sigma^{\mathrm{low}}_{\mathrm{ZA}}$ (10^5 W m^{-2} K$^{-5/2}$), $c^{\mathrm{low}}_{V,\mathrm{ZA}}$ (10^3 J m^{-3} K^{-2}).

	MoS_2	WS_2	$MoSe_2$	WSe_2	Graphene
M_{uc}	160.1	248.0	253.9	341.8	24.02
a	3.118	3.126	3.244	3.249	2.468
v_{LA}	6.84	5.73	5.20	4.66	21.7
v_{TA}	4.05	3.41	3.10	2.80	11.1
A_{ZA}	6.34	5.39	5.31	4.85	5.53
$\sigma^{\mathrm{low}}_{\mathrm{TA+LA}}$	$0.563\,T^2$	$0.670\,T^2$	$0.738\,T^2$	$0.819\,T^2$	$0.352\,T^2$
$\sigma^{\mathrm{low}}_{\mathrm{ZA}}$	$3.075\,T^{3/2}$	$3.335\,T^{3/2}$	$3.360\,T^{3/2}$	$3.516\,T^{3/2}$	$5.930\,T^{3/2}$
$c^{\mathrm{low}}_{V,\mathrm{TA+LA}}$	$0.037\,T^2$	$0.052\,T^2$	$0.064\,T^2$	$0.078\,T^2$	$0.008\,T^2$
$c^{\mathrm{low}}_{V,\mathrm{ZA}}$	$1.237\,T$	$1.455\,T$	$1.477\,T$	$1.617\,T$	$2.554\,T$

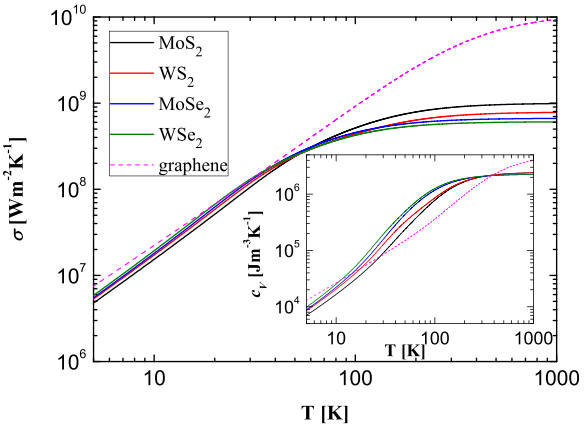

FIG. 3. The thermal conductance of monolayer TMDs and graphene as a function of temperature. The inset shows the specific heat.

$$\sigma^{\mathrm{low}}(T) = \int_0^{\infty} \frac{\partial f}{\partial T}(\hbar\omega)\rho(\omega)\frac{2}{\pi}\frac{|v(\omega)|}{2}d\omega, \tag{2}$$

and

$$c_V^{\mathrm{low}}(T) = \int_0^{\infty} \frac{\partial f}{\partial T}(\hbar\omega)\rho(\omega)d\omega, \tag{3}$$

where $\frac{2}{\pi}$ in Eq. (2) results from the angular average of velocity, and ρ is the phonon density of state per unit volume. The infinite upper limit means the integral can be applied to all phonons as the upper limit contributing to σ and c_V is automatically determined by the temperature related $\frac{\partial f}{\partial T}(\hbar\omega)$. For TA branch and LA branch, $\omega = v_{\mathrm{TA/LA}}\ q$, and thus, $\rho(\omega) = \frac{\omega}{2\pi H v^2_{\mathrm{TA/LA}}}$, then the contribution from TA branch and LA branch to the thermal conductance is

$$\sigma^{\mathrm{low}}_{\mathrm{TA/LA}}(T) = \frac{\eta_1 k_B^3}{2\pi^2\hbar^2 H}\frac{T^2}{v_{\mathrm{TA/LA}}}, \tag{4}$$

with $\eta_1 = \int_0^{\infty} x^3 e^x/(e^x-1)^2 dx \simeq 7.21$, where $x = \hbar\omega/k_BT$. The contribution from TA branch and LA branch to the specific heat is

$$c^{\mathrm{low}}_{V,\mathrm{TA/LA}}(T) = \frac{\eta_1 k_B^3}{2\pi\hbar^2 H}\frac{T^2}{v^2_{\mathrm{TA/LA}}}. \tag{5}$$

The $\sigma^{\mathrm{low}}_{\mathrm{TA/LA}}$ and $c^{\mathrm{low}}_{V,\mathrm{TA/LA}}$ have the same T^2 dependence, and differ by a factor of $\frac{1}{\pi v_{\mathrm{TA/LA}}}$. For ZA branch, $\omega = \alpha_{\mathrm{ZA}}\ q^2$, and thus, $\rho(\omega) = \frac{1}{4\pi H\alpha_{\mathrm{ZA}}}$, $v(\omega) = 2\sqrt{\alpha_{\mathrm{ZA}}\omega}$, then the contribution from ZA branch to the thermal conductance is

$$\sigma^{\mathrm{low}}_{\mathrm{ZA}}(T) = \frac{\eta_2 k_B^{5/2}}{2\pi^2\hbar^{3/2} H}\frac{T^{3/2}}{\sqrt{\alpha_{\mathrm{ZA}}}}, \tag{6}$$

with $\eta_2 = \int_0^{\infty} x^{5/2} e^x/(e^x-1)^2 dx \simeq 4.46$.[36] The contribution from ZA branch to the specific heat is

$$c^{\mathrm{low}}_{V,\mathrm{ZA}}(T) = \frac{\eta_3 k_B^2}{4\pi\hbar H}\frac{T}{\alpha_{\mathrm{ZA}}}, \tag{7}$$

with $\eta_3 = \int_0^{\infty} x^2 e^x/(e^x-1)^2 dx \simeq 3.29$.

The $c_{V,\mathrm{ZA}}^{\mathrm{low}}$ has a linear T dependence, in contrast to the T^2 dependence for TA and LA modes. The reason is that the temperature dependence of c_V^{low} is related to $\rho(\omega)$. For ZA modes, the quadratic dispersion results in constant $\rho(\omega)$, then the number of excited modes as well as $c_{V,\mathrm{ZA}}^{\mathrm{low}}$ linearly depends on T. However, for TA and LA modes, due to the linear dependence of $\rho(\omega)$ on ω, $c_{V,\mathrm{TA/LA}}^{\mathrm{low}}$ has T^2 dependence. Furthermore, because the average velocity of the excited ZA phonons also depend on $\sqrt{\omega}$, providing an extra $T^{1/2}$ dependence in the thermal conductance, $\sigma_{\mathrm{ZA}}^{\mathrm{low}}$ has $T^{3/2}$ dependence. Similarly, the constant velocities of TA and LA modes have no extra T influence, giving the same T^2 dependence for $\sigma_{\mathrm{TA/LA}}^{\mathrm{low}}$ as $c_{V,\mathrm{TA/LA}}^{\mathrm{low}}$. The c_V^{low} has the same correlation with $v_{\mathrm{TA/LA}}$ or α_{ZA} as ρ does. The lower $v_{\mathrm{TA/LA}}$ or α_{ZA}, the larger ρ and c_V^{low}. Considering that $v_{\mathrm{TA/LA}}$ and α_{ZA} approximately scale as $1/\sqrt{M_{uc}}$, the c_V^{low} increases with M_{uc}, indicating the TMDs with larger atomic mass have larger c_V^{low}, which can be seen in Fig. 3. Because σ^{low} explicitly depends on the velocity [see Eqs. (1) and (2)], the atomic mass dependence of σ^{low} is weakened. The $\sigma_{\mathrm{TA/LA}}^{\mathrm{low}}$ is proportional to $\sqrt{M_{uc}}$, and $\sigma_{\mathrm{ZA}}^{\mathrm{low}}$ is proportional to $M_{uc}^{1/4}$. In short, both c_v^{low} and σ^{low} increase with larger atomic mass. Furthermore, the atomic mass has a stronger influence on c_V^{low} and σ^{low} for the TA and LA modes than for the ZA modes.

Substituting the calculated values of α_{ZA}, v_{TA}, and v_{LA} into Eqs. (4)–(7), the low temperature asymptotic behaviors of σ^{low} and c_V^{low} are obtained. For instance, those for monolayer MoS_2 are shown in Figs. 4(a) and 4(b), in agreement with the direct calculation. The contribution to σ^{low} and c_V^{low} from TA and LA branches surpasses the contribution from the ZA branch above 30 K, and the thermal conductance and specific heat evidently deviates from $\sim T^{3/2}$ and T dependence, respectively. The low temperature asymptotic values for all monolayer TMDs are listed in Table I.

It is interesting to compare monolayer TMDs with graphene. The "by construction" approach is also imposed on the IFCs of graphene to ensure the quadratic dispersion for ZA branch, and a thickness of 3.35 Å is used, which corresponds to the layer separation of graphite.[36] The σ and c_V of graphene are also plotted in Fig. 3 for comparison. For low temperatures, the results can be found in Figs. 4(c) and 4(d) and are also listed in Table I. The calculated results are well consistent with previous studies.[36,38,40,46,47] The high temperature c_V of graphene is larger than that for monolayer TMDs by a factor of ~2, which is simply the difference of the volume per atom. For graphene, $v_{\mathrm{TA}} \simeq 11.1 \times 10^3$ m/s and $v_{\mathrm{LA}} \simeq 21.7 \times 10^3$ m/s, respectively, which are about 3–5 times larger than that of monolayer TMDs. Mainly due to much larger group velocities of TA and LA branches and partially because of smaller volume per atom, the high temperature σ of graphene is larger than that of monolayer TMDs by almost one order of magnitude. On the contrary, at low temperatures, the larger v_{TA} and v_{LA} cause $\sigma_{\mathrm{TA/LA}}^{\mathrm{low}}$ and $c_{V,\mathrm{TA/LA}}^{\mathrm{low}}$ of graphene to be several times smaller even though a smaller thickness H is used for graphene. Meanwhile, in graphene, $\alpha_{\mathrm{ZA}} \simeq 5.53 \times 10^{-7}$ m^2/s, which is close to the values of monolayer TMDs. As a result, the low temperature $c_{V,\mathrm{ZA}}^{\mathrm{low}}$ and $\sigma_{\mathrm{ZA}}^{\mathrm{low}}$ of graphene are larger than those of TMDs mainly because of the smaller thickness. Due to the dominance of ZA branch, the low temperature c_V^{low} and σ^{low} of graphene is larger. If taking the same H for graphene and TMDs, σ^{low} and c_V^{low} of these systems are then very comparable below 100 K. Much smaller contribution from TA branch and LA branch and larger contribution from ZA branch in graphene cause the ZA branch to dominate up to higher temperature than those for monolayer TMDs, as can be seen from Figs. 4(c) and 4(d).

As revealed above, the thermal conductance increases with atomic mass at low temperatures below ~50 K, while it decreases with atomic mass at high temperatures. As a consequence, the temperature dependent thermal conductance crosses at some intermediate temperature. This crossing behavior of temperature dependent thermal conductance is a

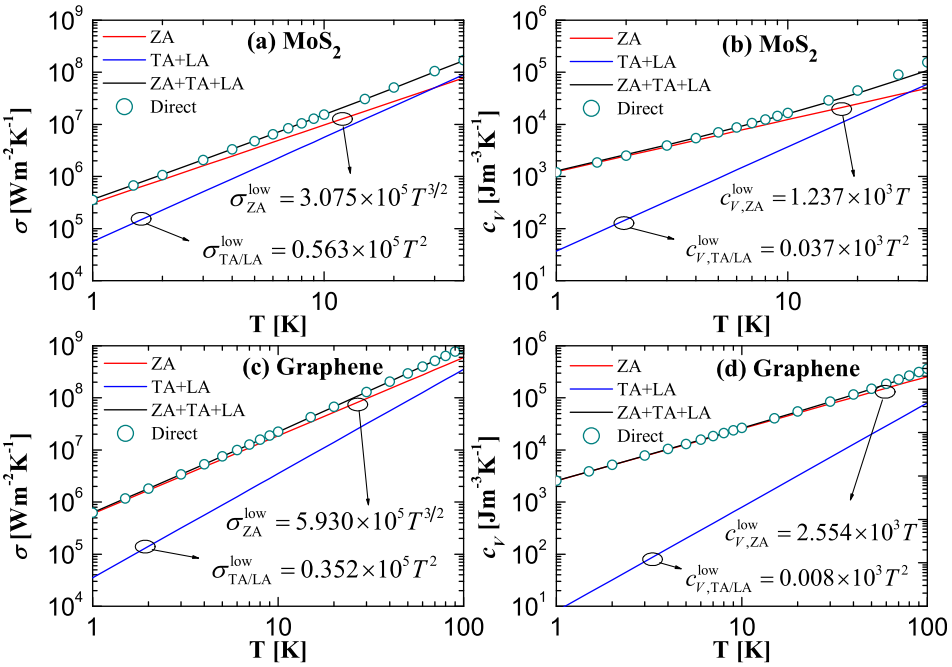

FIG. 4. The low temperature asymptotic behavior of thermal conductance and specific heat for monolayer MoS_2 and graphene using Eqs. (4)–(7). The symbols are the direct calculations in consistence with Fig. 3.

signature of the thermal conductance being influenced by atomic mass. Ideal systems of studying the effect of atomic mass on thermal conductance can be elements composed of pure but different isotopes. Then, only the mass is different, and the phonon dispersion is exactly scaled based on the mass difference of isotopes. As an example, we can consider isotopically pure graphene composed of ^{12}C and ^{13}C individually. In the low temperature limit, the $\sigma(^{12}C)/\sigma(^{13}C)$ is $\sqrt[4]{12/13} = 0.98$, while it is $\sqrt{13/12} = 1.04$ at high temperatures. Due to the small mass difference between isotopes, the effect is quite weak. Moreover, the isotopically pure samples are not easily accessible.[48] Our results demonstrate that TMDs provide a model system for studying the effect of atomic mass on the thermal conductance.

In summary, we have revealed that the thermal conductance and specific heat of monolayer TMDs are dominantly affected by the atomic mass. The thermal conductance increases with the atomic mass at low temperatures below ~50 K, while decreasing with atomic mass at high temperatures. The crossing of the temperature dependent thermal conductance is characteristic of the atomic mass effect, and TMDs provide a model system demonstrating this effect and evidencing that the thermal conductance can be effectively manipulated via the atomic mass by selecting appropriate atom. We have also clarified that due to quadratic dispersion of the ZA branch, the thermal conductance and specific heat in the low temperature limit are proportional to $T^{3/2}$ and T, respectively, in any two dimensional systems. Mainly because of much smaller group velocities of TA and LA phonons, the high temperature thermal conductances of monolayer TMDs are much smaller than that of graphene. However, due to comparable group velocities of ZA phonons, at temperatures below 100 K, thermal conductances of TMDs are rather comparable to graphene by using the same thickness.

The authors thank Dr. Natalio Mingo and Dr. Jesús Carrete for assistance and python code for the relevant IFCs calculation. J. L. Ma and X. B. Luo acknowledge supports from National Nature Science Foundation of China (Nos. 51576078 and 51376070).

[1]A. H. Castro Neto, F. Guinea, N. M. R. Peres, K. S. Novoselov, and A. K. Geim, Rev. Mod. Phys. **81**, 109 (2009).
[2]D. Krasnozhon, D. Lembke, C. Nyffeler, Y. Leblebici, and A. Kis, Nano Lett. **14**, 5905 (2014).
[3]W. S. Leong, Y. Li, X. Luo, C. T. Nai, S. Y. Quek, and J. T. L. Thong, Nanoscale **7**, 10823 (2015).
[4]Y. Xi, M. I. Serna, L. Cheng, Y. Gao, M. Baniasadi, R. Rodriguez-Davila, J. Kim, M. A. Quevedo-Lopez, and M. Minary-Jolandan, J. Mater. Chem. C **3**, 3842 (2015).
[5]H. S. Lee, S.-W. Min, Y.-G. Chang, M. K. Park, T. Nam, H. Kim, J. H. Kim, S. Ryu, and S. Im, Nano Lett. **12**, 3695 (2012).
[6]C. Lan, C. Li, Y. Yin, and Y. Liu, Nanoscale **7**, 5974 (2015).
[7]J. D. Yao, Z. Q. Zheng, J. M. Shao, and G. W. Yang, Nanoscale **7**, 14974 (2015).
[8]R. S. Sundaram, M. Engel, A. Lombardo, R. Krupke, A. C. Ferrari, P. Avouris, and M. Steiner, Nano Lett. **13**, 1416 (2013).
[9]G. Eda, H. Yamaguchi, D. Voiry, T. Fujita, M. Chen, and M. Chhowalla, Nano Lett. **11**, 5111 (2011).
[10]X. H. Wang, J. Q. Ning, C. C. Zheng, B. R. Zhu, L. Xie, H. S. Wu, and S. J. Xu, J. Mater. Chem. C **3**, 2589 (2015).
[11]W. Li, J. Carrete, and N. Mingo, Appl. Phys. Lett. **103**, 253103 (2013).
[12]I. Jo, M. T. Pettes, E. Ou, W. Wu, and L. Shi, Appl. Phys. Lett. **104**, 201902 (2014).
[13]J. Liu, G.-M. Choi, and D. G. Cahill, J. Appl. Phys. **116**, 233107 (2014).
[14]X. Gu and R. Yang, Appl. Phys. Lett. **105**, 131903 (2014).
[15]G. Chen, Phys. Rev. B **57**, 14958 (1998).
[16]T. Markussen, A.-P. Jauho, and M. Brandbyge, Nano Lett. **8**, 3771 (2008).
[17]J. Lee, J. Lim, and P. Yang, Nano Lett. **15**, 3273 (2015).
[18]G. Kresse and J. Furthmüller, Phys. Rev. B **54**, 11169 (1996).
[19]P. E. Blöchl, Phys. Rev. B **50**, 17953 (1994).
[20]J. P. Perdew and A. Zunger, Phys. Rev. B **23**, 5048 (1981).
[21]A. Togo, F. Oba, and I. Tanaka, Phys. Rev. B **78**, 134106 (2008).
[22]W. Li, J. Carrete, N. A. Katcho, and N. Mingo, Comput. Phys. Commun. **185**, 1747 (2014).
[23]C. Ataca, M. Topsakal, E. Aktürk, and S. Ciraci, J. Phys. Chem. C **115**, 16354 (2011).
[24]A. Molina-Sánchez and L. Wirtz, Phys. Rev. B **84**, 155413 (2011).
[25]K. Kaasbjerg, K. S. Thygesen, and K. W. Jacobsen, Phys. Rev. B **85**, 115317 (2012).
[26]Y. Ge and A. Y. Liu, Phys. Rev. B **87**, 241408 (2013).
[27]H. Xie, M. Hu, and H. Bao, Appl. Phys. Lett. **104**, 131906 (2014).
[28]X. Gu and R. Yang, J. Appl. Phys. **117**, 025102 (2015).
[29]N. D. Drummond, V. Zólyomi, and V. I. Fal'ko, Phys. Rev. B **85**, 075423 (2012).
[30]E. Scalise, M. Houssa, G. Pourtois, B. van den Broek, V. Afanas'v, and A. Stesmans, Nano Res. **6**, 19 (2013).
[31]G. Qin, Q.-B. Yan, Z. Qin, S.-Y. Yue, M. Hu, and G. Su, Phys. Chem. Chem. Phys. **17**, 4854 (2015).
[32]A. Jain and A. J. H. McGaughey, Sci. Rep. **5**, 8501 (2015).
[33]Z. Zhu and D. Tománek, Phys. Rev. Lett. **112**, 176802 (2014).
[34]R. Fei, A. Faghaninia, R. Soklaski, J.-A. Yan, C. Lo, and L. Yang, Nano Lett. **14**, 6393 (2014).
[35]J. Carrete, W. Li, L. Lindsay, D. A. Broido, and N. Mingo, "Physically meaningful force constants, and the phonon dispersion of few-layered materials" (unpublished).
[36]N. Mingo and D. A. Broido, Phys. Rev. Lett. **95**, 096105 (2005).
[37]W. Li and N. Mingo, J. Appl. Phys. **114**, 054307 (2013).
[38]J.-W. Jiang, J.-S. Wang, and B. Li, Phys. Rev. B **79**, 205418 (2009).
[39]A. Mizel, L. X. Benedict, M. L. Cohen, S. G. Louie, A. Zettl, N. K. Budraa, and W. P. Beyermann, Phys. Rev. B **60**, 3264 (1999).
[40]V. N. Popov, Phys. Rev. B **66**, 153408 (2002).
[41]R. A. Gordon, D. Yang, E. D. Crozier, D. T. Jiang, and R. F. Frindt, Phys. Rev. B **65**, 125407 (2002).
[42]T. Böker, R. Severin, A. Müller, C. Janowitz, R. Manzke, D. Voß, P. Krüger, A. Mazur, and J. Pollmann, Phys. Rev. B **64**, 235305 (2001).
[43]N. Wakabayashi, H. G. Smith, and R. M. Nicklow, Phys. Rev. B **12**, 659 (1975).
[44]W. Schutte, J. D. Boer, and F. Jellinek, J. Solid State Chem. **70**, 207 (1987).
[45]P. Giannozzi, S. de Gironcoli, P. Pavone, and S. Baroni, Phys. Rev. B **43**, 7231 (1991).
[46]E. Pop, V. Varshney, and A. K. Roy, MRS Bull. **37**, 1273 (2012).
[47]E. Muñoz, J. Lu, and B. I. Yakobson, Nano Lett. **10**, 1652 (2010).
[48]S. Chen, Q. Wu, C. Mishra, J. Kang, H. Zhang, K. Cho, W. Cai, A. A. Balandin, and R. S. Ruoff, Nat. Mater. **11**, 203 (2012).